Supplemental Information

Conformational Transitions that Enable Histidine Kinase Autophosphorylation and Receptor Array Integration

Anna R. Greenswag, Alise Muok, Xiaoxiao Li, and Brian R. Crane

Department of Chemistry and Chemical Biology, Cornell University, Ithaca, NY 14853 USA

SI Figures

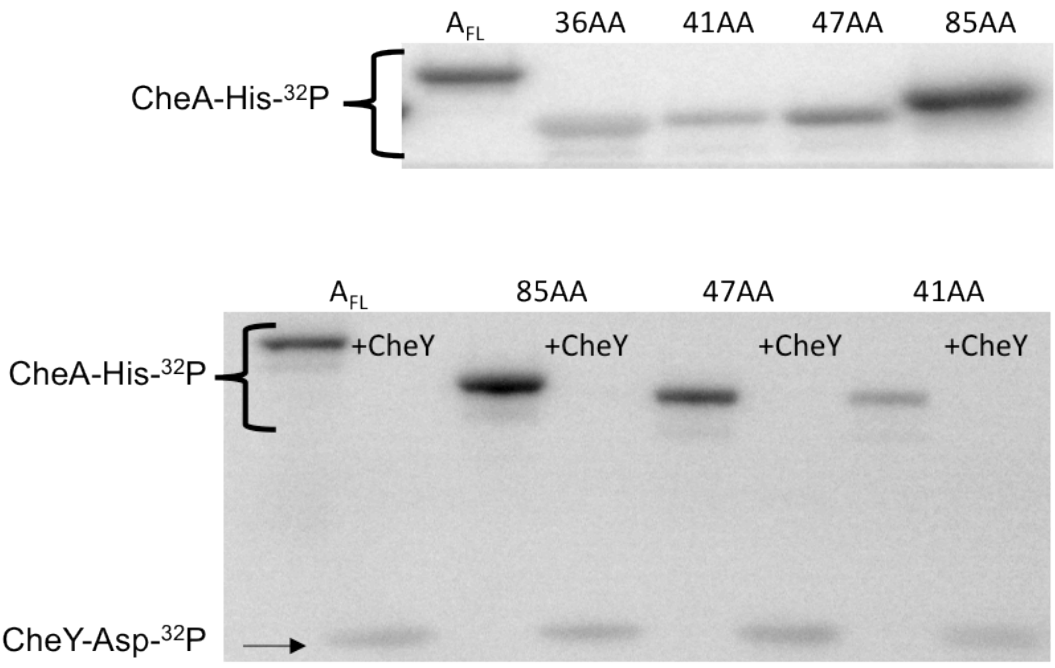

Figure S1. **Phosphorylation activities of ΔP2 variants.** Phosphorimages of $CheA_{FL}$ and ΔP2 variants showing autophosphorylation activity (above) and CheY phosphotransfer activity (below). Bottom gel shows ± CheY in alternating lanes.

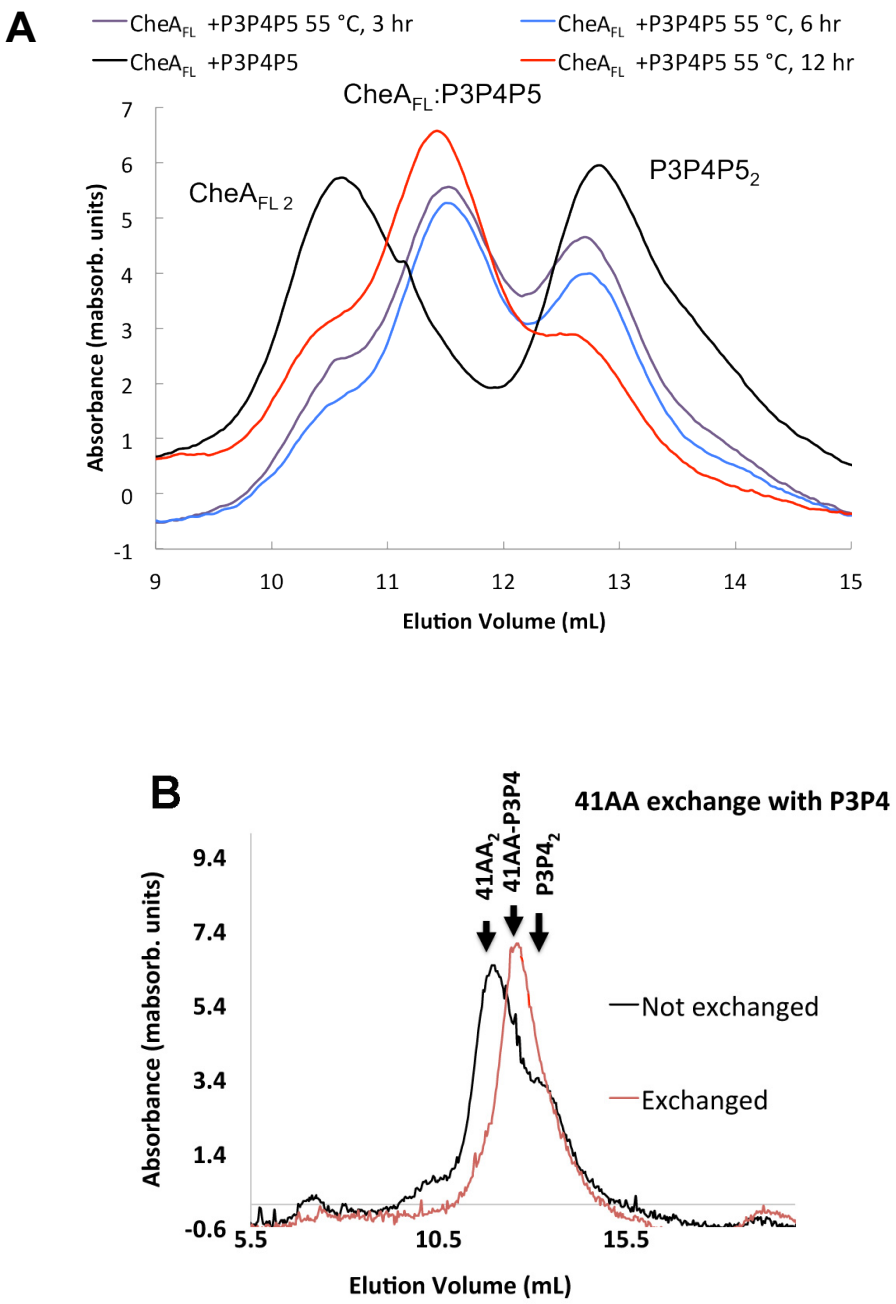

Figure S2. **Subunit of exchange CheA$_{FL}$ with P3P4P5 (A) and 41AA with P3P4 (B).** (A) SEC profiles of CheA$_{FL}$ (35 mM) and P3P4P5 (35 mM) dimers during heat exchange at 55 °C at 0 hours (black curve), 3 hours (purple curve), 6 hours (purple curve) and 12 hours (red curve). The sample exchanges to a mixture of CheA$_{FL\ 2}$:(CheA$_{FL}$:P3P4P5):P3P4P5$_2$ in a roughly 1:2:1 ratio. (B) SEC profiles of 41AA mixed with P3P4 before (black curve) and after (red curve) subunit exchange for 12 hrs at 55 °C. P3P4 was used instead of P3P4P5 to distinquish the 41AA homodimer, which is smaller than CheA$_{FL}$ from the heterodimer.

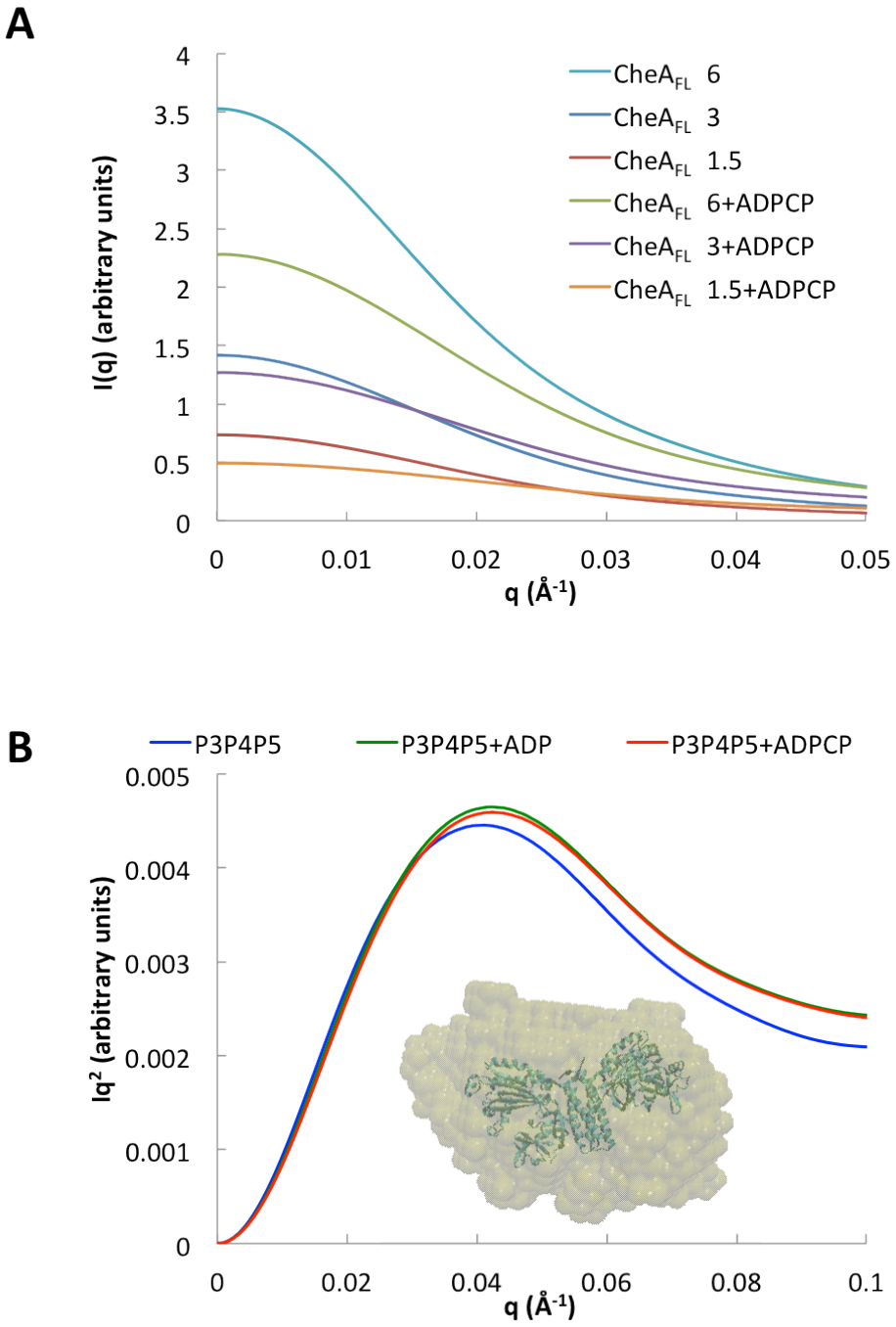

Figure S3. **SAXS of CheA$_{FL}$ and P3P4P5. A:** Intensity vs. scattering plot of CheA$_{FL}$ at various concentrations as indicated (6, 3, 1.5 mg/mL) with and without ADPCP (5 mM). Curves are shown after smoothing and regularization. **B:** Kratky plot of P3P4P5 (6 mg/mL) with and without nucleotide: ADP and ADPCP (both at 5 mM). Inset shows molecular envelope calculated from SAXS data with a superimposed dimer of P3P4P5 as a ribbon diagram.

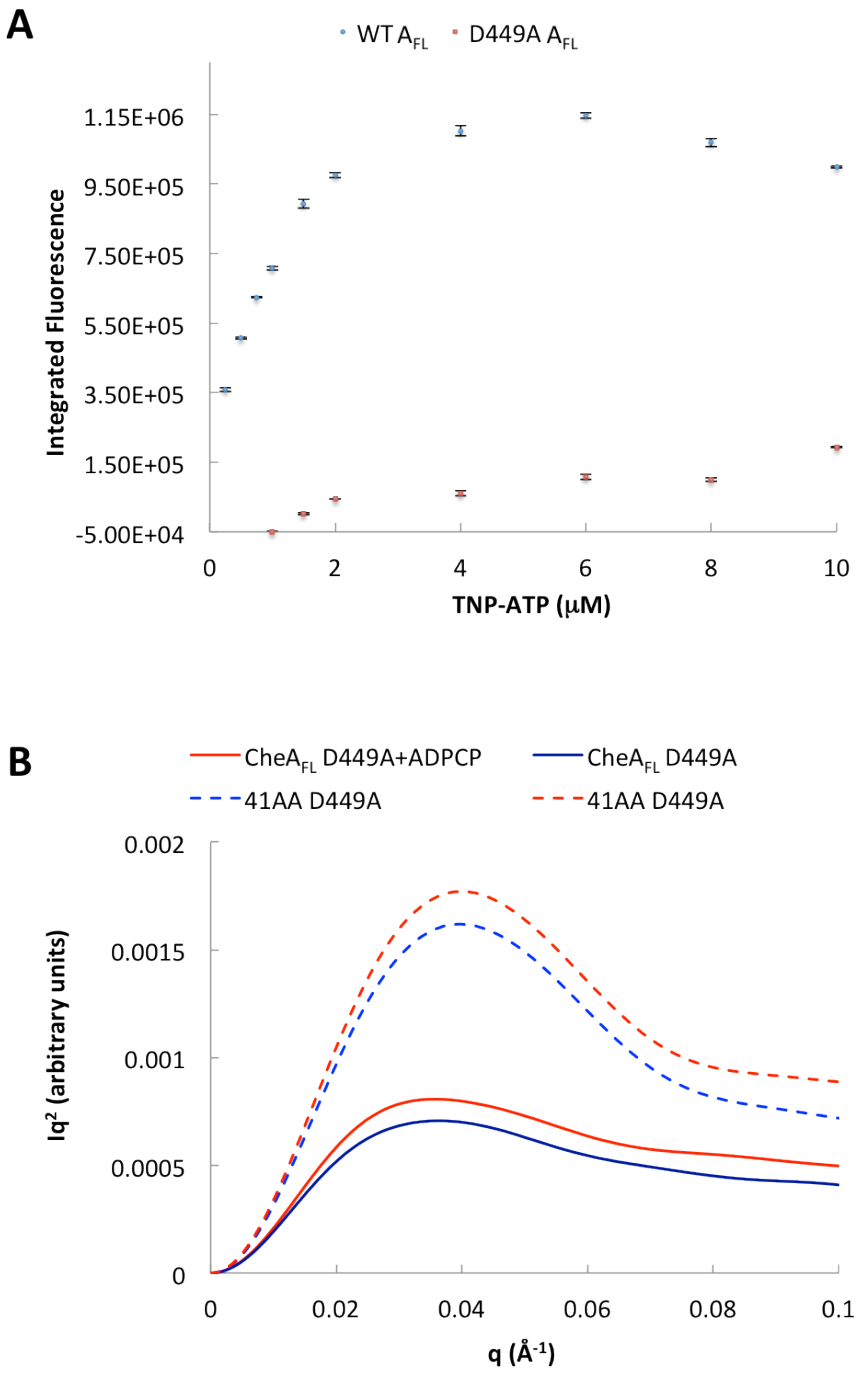

Figure S4. **Lack of nucleotide binding and SAXS changes in the CheA D449A mutant. (A)** Binding isotherms of fluorescent TNP-ATP to WT $CheA_{FL}$ and D449A $CheA_{FL}$ (each at 2 μM). WT CheA shows a large increase in fluorescence upon binding TNP-ATP, which is nearly absent in the mutant. WT data was corrected by a non-binding blank but not by any inner filter effects. (**B)** SAXS Kratky plots of $CheA_{FL}$ D449A and 41AA D449A (20 μM) with and without nucleotide. Addition of ADPCP (5 mM) shows no change in globular shape of either $CheA_{FL}$ or 41AA with the D449A substitution.

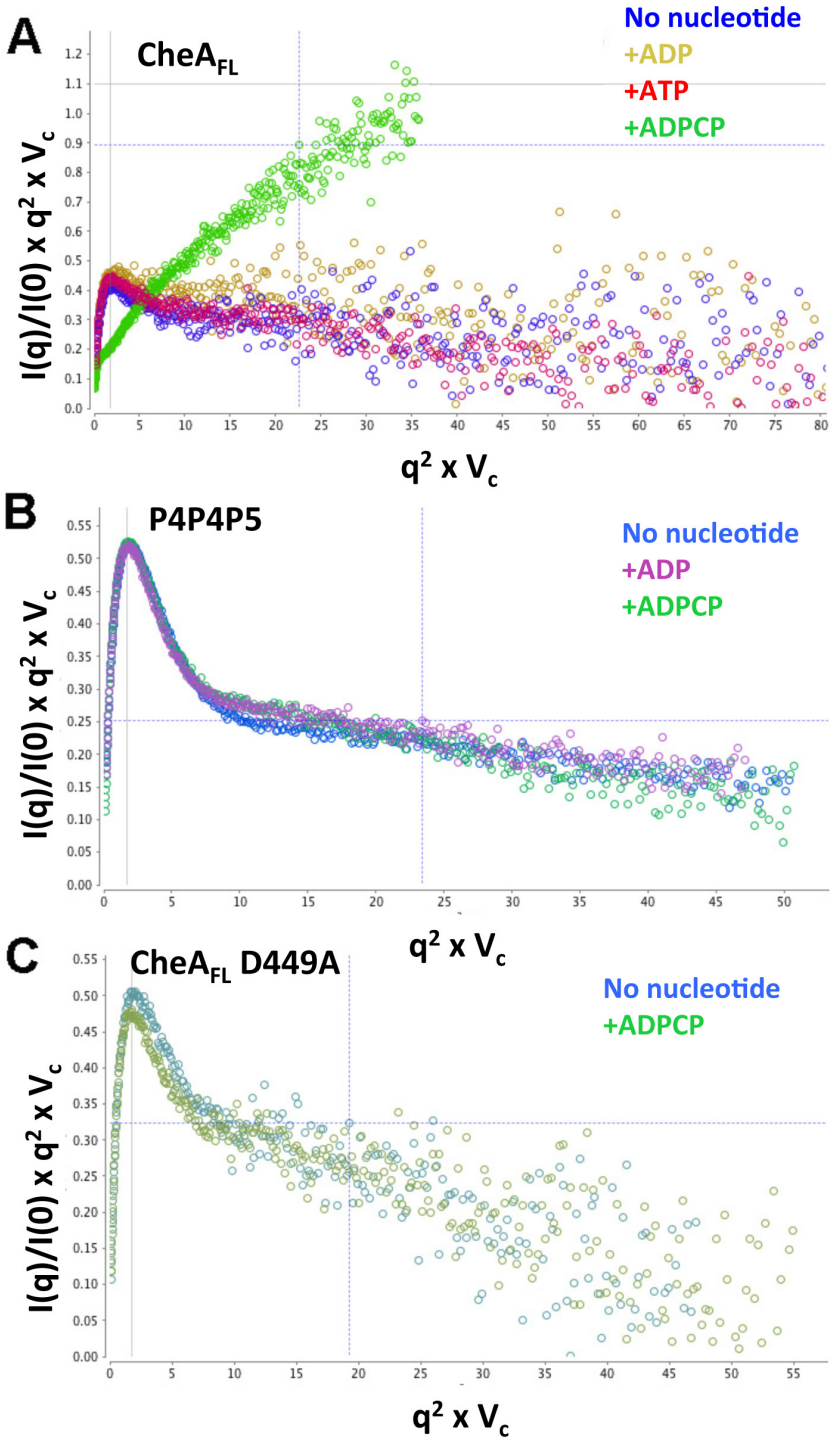

Figure S5. **Dimensionless Kratky analysis.** Curves plotted as I(q)/I(0) x q^2 x V_C vs q^2 x V_C, where V_C is the volume-per-correlation length. For compact particles, peak height is directly proportional to V_C/Rg^2, which is inversely proportional to the surface-to-volume ratio of the particle. Data is shown for **(A)** $CheA_{FL}$ with nucleotides as indicated, **(B)** P3P4P5 and **(C)** $CheA_{FL}$ D449A, a nucleotide binding deficient mutant. Only ADPCP bound in the P4 ATP-pocket of the full-length enzyme produces a more flexible conformation. Vertical solid lines mark peaks.

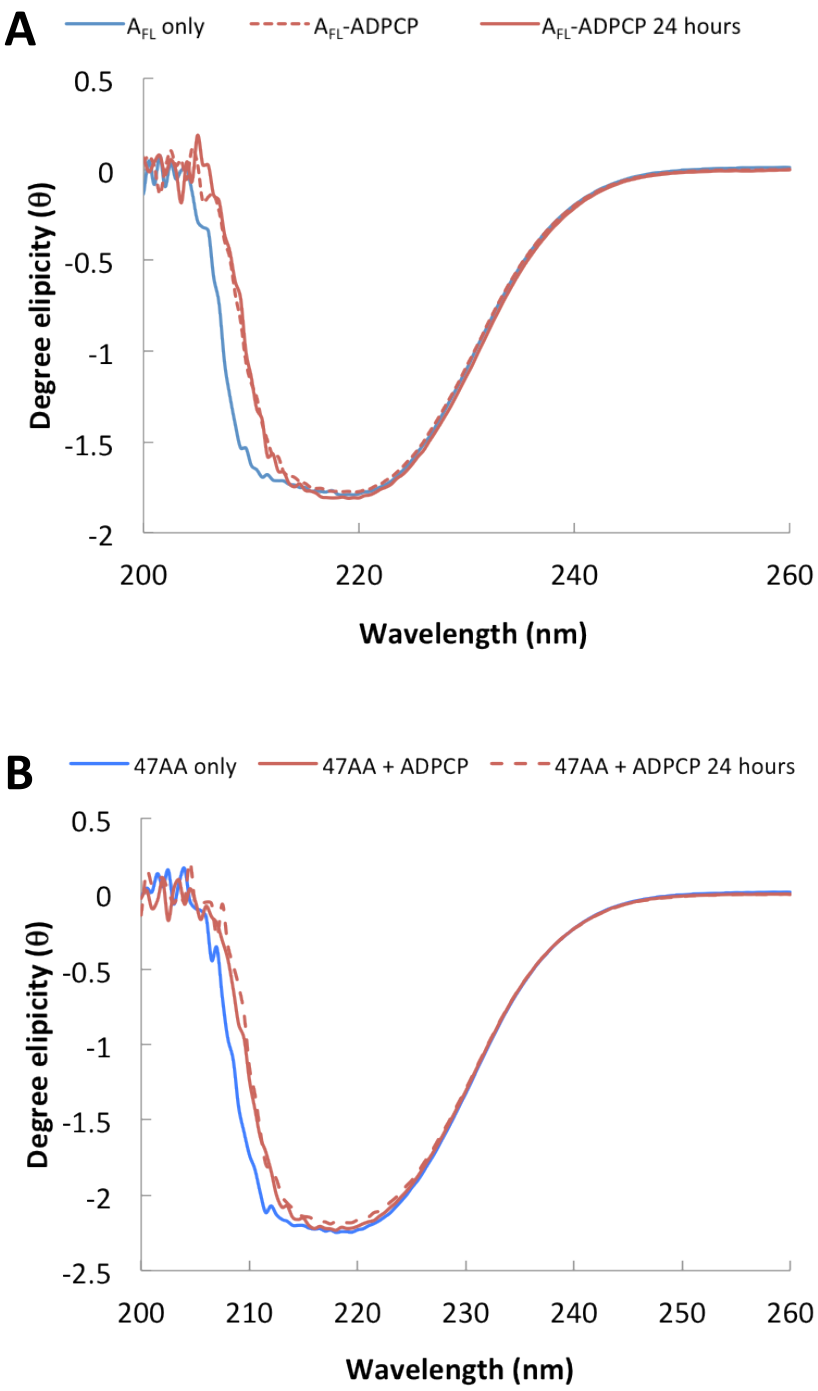

Figure S6. **CD spectra of $CheA_{FL}$ (A) and 47AA (B) with and without ADPCP.** Circular dichroism spectra of $CheA_{FL}$ and 47AA (0.5 mg/mL) before (blue) and after (red dashed) addition of ADPCP (1 mM) show no change in helical content. Another spectrum collected 24 hours after ADPCP addition shows no long-term effects (red solid). Note that there is a baseline shift upon addition of the nucleotide due to phosphate [1].

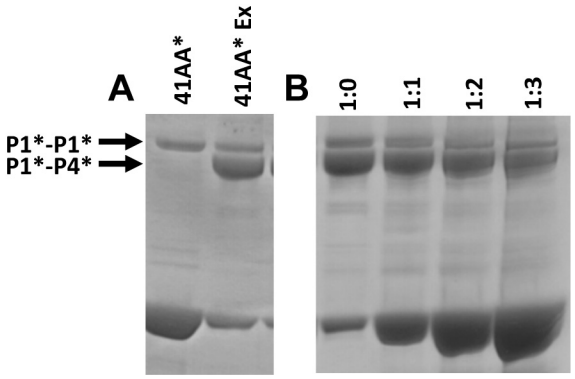

Figure S7**. Cross-linking patterns of 41AA.** (**A**) SDS-page gel of 41AA* (P1*P4*) double cys mutant before (41AA*) and after (41AA*) subunit exchange and cross-linking. The P1*-P1* cross-linked band is observed on purification of the double mutant. (**B**) SDS-page gel of 41AA* (P1*P4*) double cys mutant mixed with WT 41AA after 12 hours of 55 °C subunit exchange, and 1 hr incubation with initiator. Lane 1 41AA*:41AA = 1:0 molar ratio; Lane 2: 41AA*:41AA = 1:1; Lane 3: 41AA*:41AA = 2:1; Lane 4: 41AA*:41AA = 2:1. There is no change in cross-linking pattern with increased WT subunits, which indicates that the P1*-P4* cross-link occurs within the same subunit.

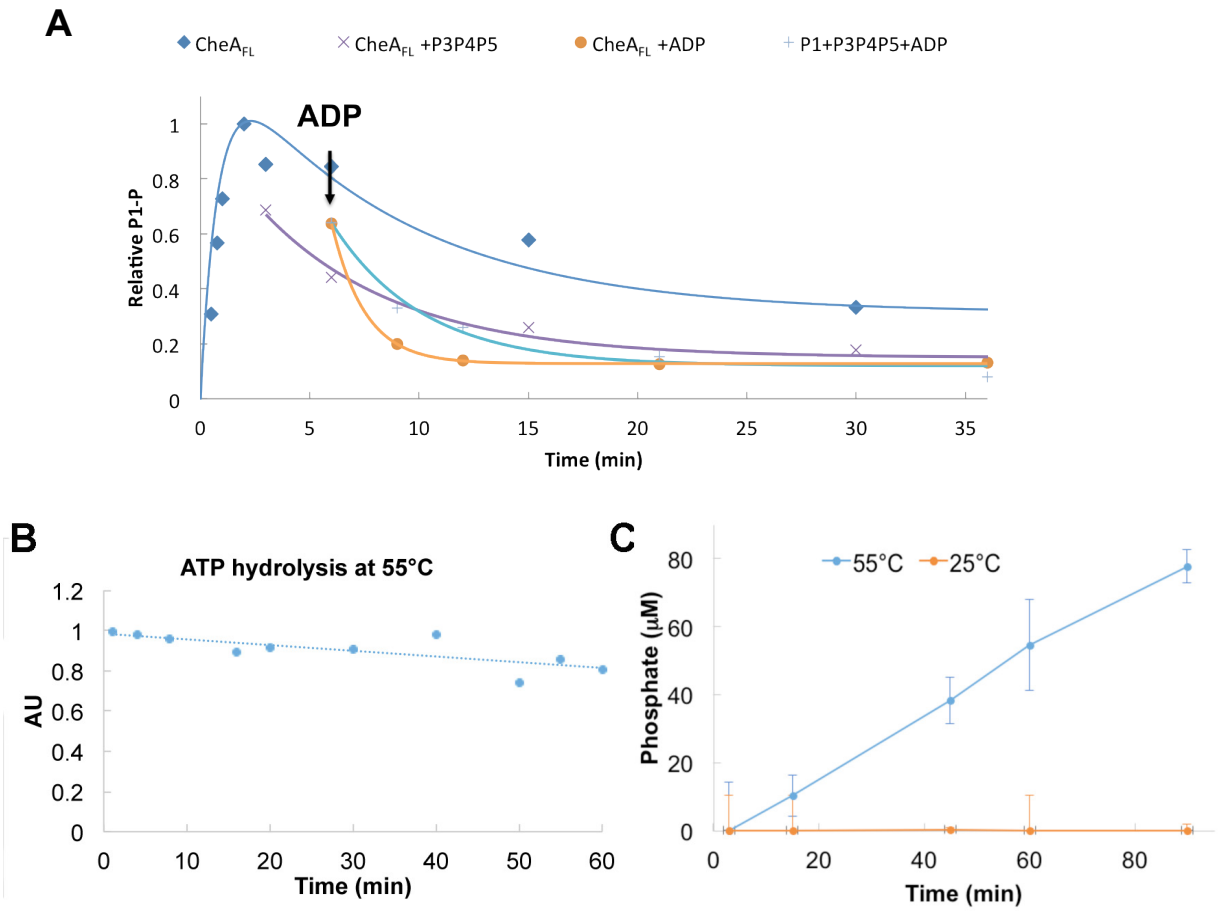

Figure S8. **Assessment of CheA$_{FL}$ Phosphatase Activity (A)** Addition of ADP to CheA$_{FL}$ and separated domains deplete P1-P. Time courses for autophosphorylation activity of CheA (10 mM) and separated domains at 55 °C. After 6 minutes of initial exposure to ^{32}P-ATP, cold ADP (2 mM) was added to promote dephosphorylation of His-P. Both CheA$_{FL}$-P and P1-P of the separated domains decrease after addition of cold ADP. Addition of kinase in the form of P3P4P5 to CheA$_{FL}$ does not increase phoshorylation of CheA$_{FL}$. (B) Evaluation of ATP hydrolysis in the absence of enzyme under reaction conditions for CheA autophosphorylation at 55 °C. ADP production was measured by an enzyme coupled assay that detects loss of NADH by spectrophotometric means (see Materials and Methods); the remaining ATP is shown relative to initial conditions. Small amounts of ADP production were confirmed by thin-layer chromatography (not shown). (C) Phosphatase activty of CheA$_{FL}$ at 25 °C and 55 °C as measured by release of inorganic phosphate and detection by complexation with the Biomol Green reagent (Enzo Life Sciences, BML-AK111; see Materials and Methods). CheA$_{FL}$ only shows phosphatase activity at elevated temperature.

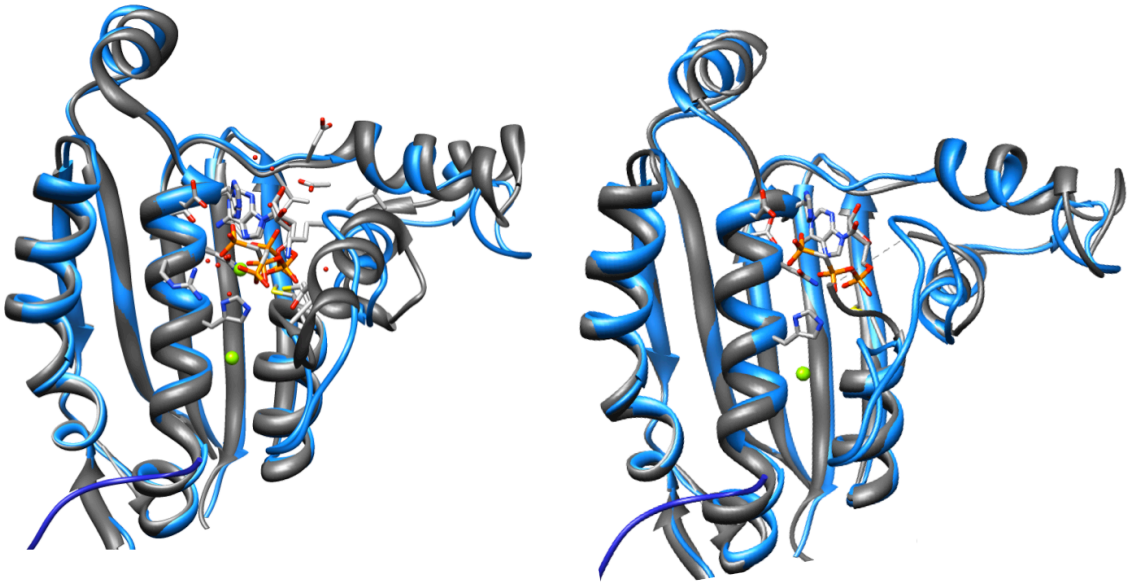

Figure S9**. Overlay of P3P4 kinase domain with existing crystal structures.** Kinase domain superpositions of P4 [2] (left) and P3P4P5 [3] (right) on P4 from the P3P4 structure (blue).

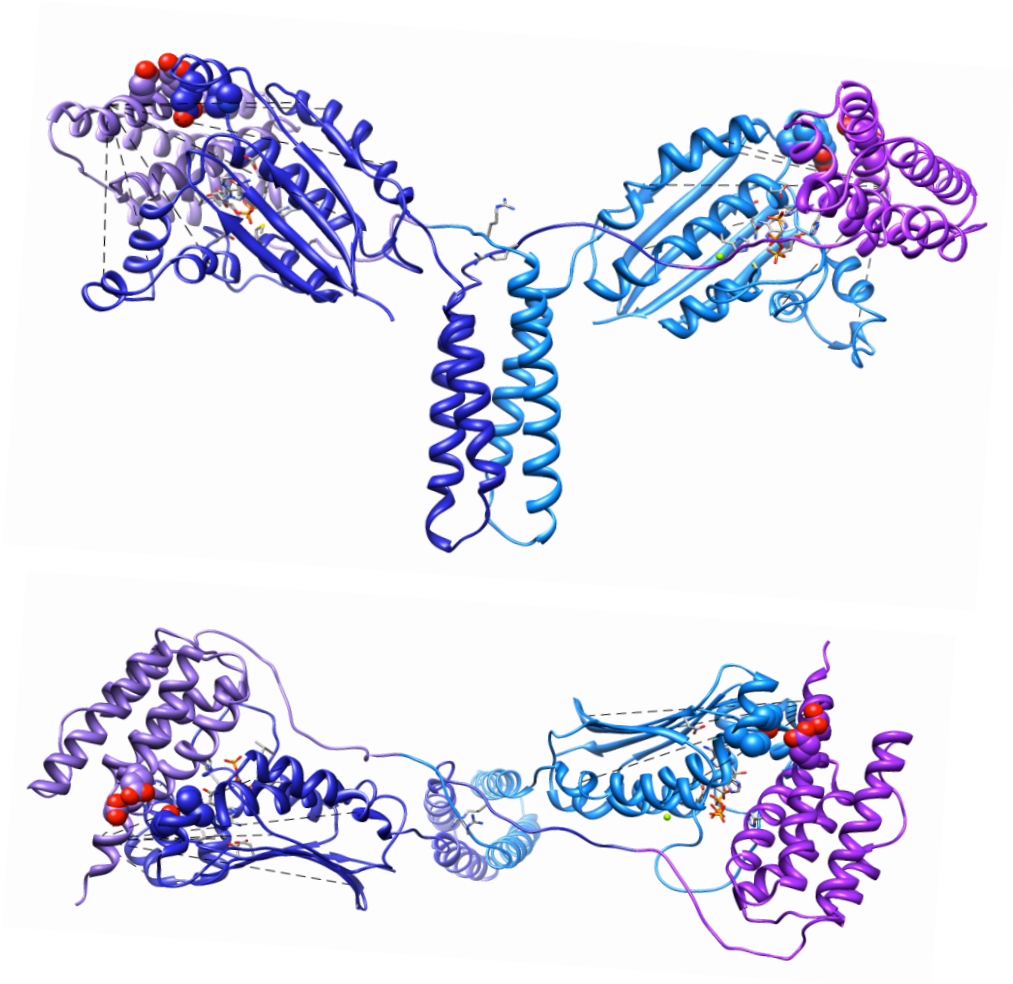

Figure S10. **Spatial constraints for modeling a P1-P4 interaction.** P1 was placed next to P4 such that residues whose mutations affect P1-P4 interactions were close (shown as spheres: Asp11, Glu15, Pro417, Glu420) [4] and residues that cross-link when changed to Cys were within 11 Å (dotted lines: Gly7 to Asn363, Asp371, Asn381, Arg437, Ala476, and Asn484) [5]. Additional constraints include the 47AA linker having the minimal linker length for transphosphorylation and close proximity of the P1 substrate His to the position of the ATP-γ-phosphate and S492.

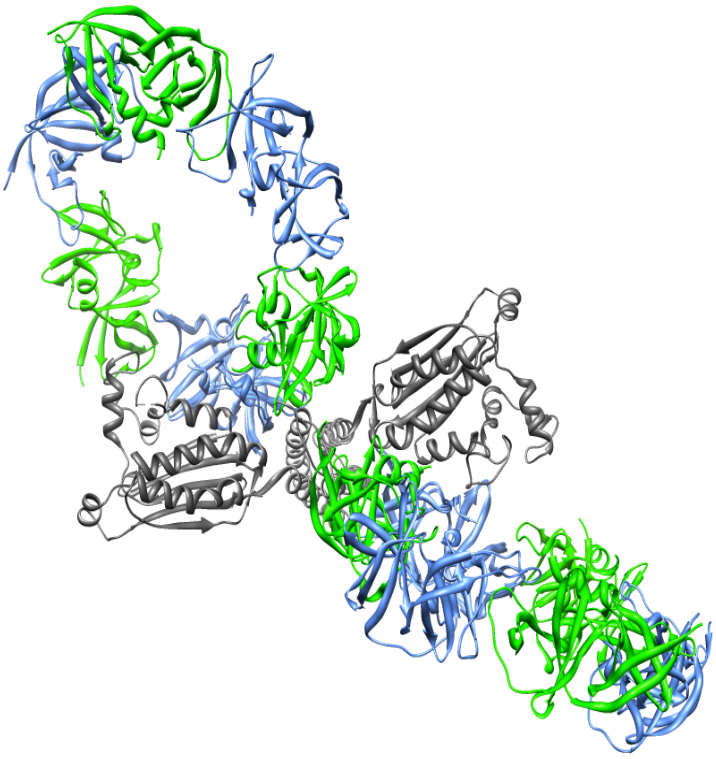

Figure S11**. Ring juxtapositoin predicted by the P3P4P5 crystal structure.** Orientation of the CheW/P5 [6] rings formed by the P3-P4 juxtaposition in the P3P4P5 structure [3] is not compatible with a planar extended array due to the P3-P4 linker conformation in P3P4P5.

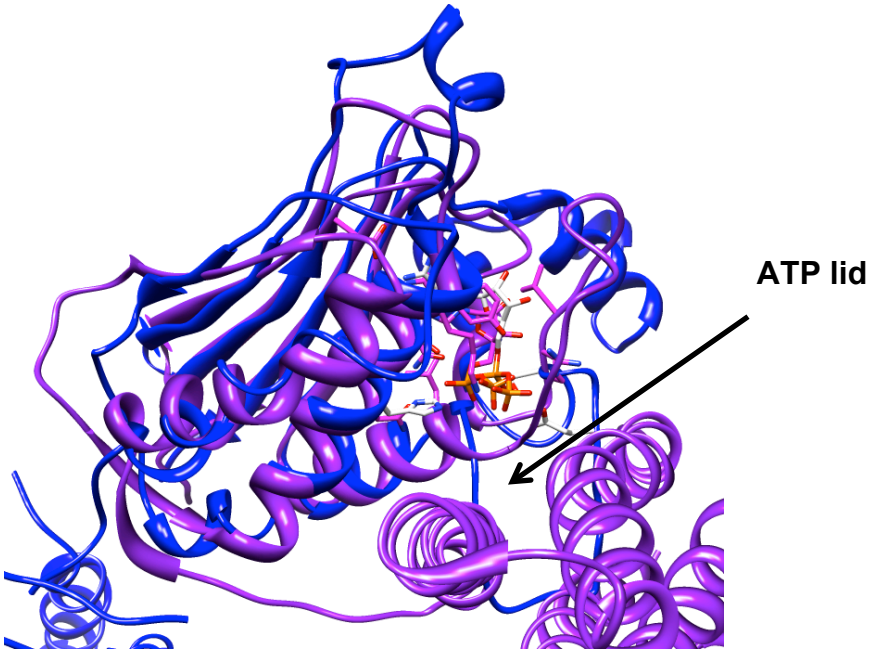

Figure S12. **Comparison of the sensor kinase substrate complex to the P1-P4 complex.** Superposition of the kinase domains of 3DGE [7] (purple) and P4 (blue) show that the ATP-lid of CheA would clash with the sensor kinase dimerization domain, on which the substrate His resides.

The effect of covalent tethering of P1 and the P1-to-P3 linker length on CheA activity assuming a Gaussian chain model.

Here we consider how tethering P1 to the CheA kinase unit (P3P4 or P3P4P5) will affect the relative rates of autophosphorylation compared to the bimolecular reaction between the two separated species. The analysis below follows Wang and Davidson [8] and Hagen and Eaton [9].

Consider the unimolecular autophosphorylation reaction of $CheA_{FL}$:

$$CheA^O \overset{k_c/k_o}{\Longleftrightarrow} CheA^C \overset{k_{cat}}{\longrightarrow} CheA\text{-}P$$

Where $CheA^O$ and $CheA^C$ are the open and closed states of CheA, respectively, with the latter representing P1 associated with P3P4 in a complex competent for autophosphorylation. If $k_{cat} <<< k_c, k_o$ then the overall rate constant for production of CheA-P is k_{cat} weighted by the equilibrium constant for P1 closure (K^{uni}):

$$K^{uni} = \frac{k_c}{k_o} = \frac{[CheA^C]}{[CheA^O]} \text{ or } K^{uni} \cdot [CheA^o] = [CheA^C]$$

$$\frac{d[CheA\text{-}P]}{dt} = k_{cat} \cdot [CheA^C]$$

$$\frac{d[CheA\text{-}P]}{dt} = k_{cat} \cdot K^{uni} \cdot [CheA^O]$$

For the bimolecular reaction where P1 is separated from P3P4 (or P3P4P5):

$$P1 + P4 \overset{k_{on}/k_{off}}{\Longleftrightarrow} [P1\text{-}P3P4] \overset{k_{cat}}{\longrightarrow} P1\text{-}P$$

$$K^{bi} = \frac{k_{on}}{k_{off}} = \frac{[P1\text{-}P3P4]}{[P1][P3P4]} \text{ or } K^{bi} \cdot [P1][P3P4] = [P1\text{-}P3P4]$$

$$\frac{d[P1\text{-}P]}{dt} = k_{cat} \cdot K^{bi} \cdot [P1][P3P4]$$

In this case, the reaction is pseudo first order because P3P4 is not depleted during the reaction. Hence, [P3P4] = constant and the reaction is first order in the substrate [P1]. [P1] is analogous to [CheA^{O}] in the unimolecular case – but the rate expression will have an additional concentration term, [P3P4], that will cancel the reciprocal concentration units of K^{bi}.

For the unimolecular reaction we replace K^{uni} with $K^{bi}j$; where j is an effective concentration of P1 near P3P4 in the covalently tethered enzyme. j has concentration units that will cancel the reciprocal concentration units of K^{bi} and generate a unimolecular dimensionless equilibrium constant.

j is known as the Jacobson-Stockmayer factor [10] and is the probability density or concentration of one end of a chain in the vicinity of the other. We further assume that when the linker length is zero P1 is positioned to phosphorylate P4.

$$j = \left(\frac{3}{2\pi < r^2 >}\right)^{3/2}$$

where $\langle r^2 \rangle$ = average squared separation of the chain length.

From Flory [11];

$$\langle r^2 \rangle = C_n \cdot n \cdot l^2,$$

where n = number of residues in the linker, l = the unit length (3.8 Å for a Ca-Ca separation), and C_n equals the Flory characteristic ratio, which depends on the type of polymer and represents how much the chain expands due to internal constraints compared to a freely jointed chain (C_n ~ 8 for proteins in denaturant (9.5 for poly L-Ala).

(Note: To convert j from units of molecules/Å^3 to moles/L: 1.66 x 10^3 M = 1 molecule / Å^3 [10^{-27} L = 1 Å^3])

Thus, the overall effective rate constants for P1 phosphorylation in the unimolecular and biomolecular cases can be compared as:

$$k^{uni} = k_{cat} \cdot K^{bi} \cdot j$$

$$k^{bi} = k_{cat} \cdot K^{bi} \cdot [P3P4]$$

Each corresponding rate of autophosphorylation is then obtained by multiplying the above rate constants by [P1], either in the context of covalent CheA (unimolecular) or as a separate domain (bimolecular).

The ratio of j / [P3P4] determines the rate enhancement for the uni-compared to the bi-molecular reaction.

j depends upon n, the chain length, which we estimate for the various DP2 variants. Assuming that the 5^{th} helix of P1 (as found in the NMR structure) ends the P1 domain at residue 128, we take P3 to begin at residue 290, and the number of residues intervening 128 and 290 then form n. (Note, that zero linker length may in fact be detrimental to CheA autophosphorylation, but extending the linker by a few residues will not alter the spirit of the argument.). In the case of $CheA_{FL}$ the presence of the P2 domain must be taken into account. There are 262 residues between 128 and 290 but 85 of these compose the P2 domain, whose N- and C- termini are fairly close in space. Thus for the sake of simplicity, we approximate the entire P2 domain to be a single unit (n = 77 for $CheA_{FL}$).

Note that [P3P4] is an equilibrium free kinase concentration. We assume that the total concentrations of P1 and P3P4 are far below $1/K^{bi}$, such that [P3P4] ~ $[P3P4]_{Total}$.

With these considerations:

Linker	n	$<r^2>$	j (molec/Å^3)	j or [P3P4]
36AA	5	580	2.36×10^{-5}	39 mM
41AA	11	1276	7.24×10^{-6}	12 mM
47AA	16	1856	4.12×10^{-6}	6.8 mM
85AA	54	6264	6.66×10^{-7}	1.1 mM
90AA	59	6844	5.83×10^{-7}	0.97 mM
$CheA_{FL}$	77	8895	3.93×10^{-7}	0.65 mM
P1 + P3P4				0.01 mM*

*Standard reaction conditions

Thus, the random chain model would predict that $CheA_{FL}$ should be 65x more active than the separated domains under the conditions tested, and 36AA 4000x more active. These ratios of activity are in fact very different from what is found, in particular the short chains do not increase CheA activity anywhere near the level predicted by this model. Thus, domain interactions within the CheA dimer must govern autophosphorylation activity in the full-length enzyme.

As a final note, if closing of P1 to P4 in full-length enzyme was not fast compared to k_{cat}, then $1/k^{uni} = 1/k_{Dc} + 1/K^{uni}\ k_{cat,}$ where k_{Dc} is the diffusion controlled rate constant for closing.

References

[1] Kelly SM, Jess TJ, Price NC. How to study proteins by circular dichroism. Biochim Biophys Acta 2005;1751:119–39. doi:10.1016/j.bbapap.2005.06.005.

[2] Bilwes AM, Quezada CM, Croal LR, Crane BR, Simon MI. Nucleotide binding by the histidine kinase CheA. Nat Struct Mol Biol 2001;8:353–60. doi:10.1038/86243.

[3] Bilwes AM, Alex LA, Crane BR, Simon MI. Structure of CheA, a Signal-Transducing Histidine Kinase. Cell 1999;96:131–41. doi:10.1016/S0092-8674(00)80966-6.

[4] Nishiyama S, Garzón A, Parkinson JS. Mutational Analysis of the P1 Phosphorylation Domain in Escherichia coli CheA, the Signaling Kinase for Chemotaxis. J Bacteriol 2014;196:257–64. doi:10.1128/JB.01167-13.

[5] Bass RB, Butler SL, Chervitz SA, Gloor SL, Falke JJ. Use of site-directed cysteine and disulfide chemistry to probe protein structure and dynamics: Applications to soluble and transmembrane receptors of bacterial chemotaxis. Two-Compon. Signal. Syst. Pt B, vol. 423, 2007, p. 25–51.

[6] Li X, Fleetwood AD, Bayas C, Bilwes AM, Ortega DR, Falke JJ, et al. The 3.2 Å Resolution Structure of a Receptor:CheA:CheW Signaling Complex Defines Overlapping Binding Sites and Key Residue Interactions within Bacterial Chemosensory Arrays. Biochemistry 2013;52:3852–65. doi:10.1021/bi400383e.

[7] Casino P, Rubio V, Marina A. Structural Insight into Partner Specificity and Phosphoryl Transfer in Two-Component Signal Transduction. Cell 2009;139:325–36. doi:10.1016/j.cell.2009.08.032.

[8] Wang JC, Davidson N. On the probability of ring closure of lambda DNA. J Mol Biol 1966;19:469–82. doi:10.1016/S0022-2836(66)80017-7.

[9] Hagen SJ, Hofrichter J, Szabo A, Eaton WA. Diffusion-limited contact formation in unfolded cytochrome c: estimating the maximum rate of protein folding. Proc Natl Acad Sci 1996;93:11615–7.

[10] Jacobson H, Stockmayer WH. Intramolecular Reaction in Polycondensations. I. The Theory of Linear Systems. J Chem Phys 1950;18:1600–6. doi:10.1063/1.1747547.

[11] Gordon M. Statistical mechanics of chain molecules. P. J. Flory, pp. xix + 432, 1969. New York: Interscience. 164s. Br Polym J 1970;2:302–3. doi:10.1002/pi.4980020511.